
Proximal Policy Gradient Arborescence for Quality Diversity Reinforcement Learning

Sumeet Batra

University of Southern California
Los Angeles, CA 90089
ssbatra@usc.edu

Bryon Tjanaka

University of Southern California
Los Angeles, CA 90089
tjanaka@usc.edu

Matthew C. Fontaine

University of Southern California
Los Angeles, CA 90089
mfontain@usc.edu

Aleksei Petrenko

University of Southern California
Los Angeles, CA 90089
petrenko@usc.edu

Stefanos Nikolaidis

University of Southern California
Los Angeles, CA 90089
nikolaid@usc.edu

Gaurav Sukhatme

University of Southern California
Los Angeles, CA 90089
gaurav@usc.edu

Abstract

Training generally capable agents that perform well in unseen dynamic environments is a long-term goal of robot learning. Quality Diversity Reinforcement Learning (QD-RL) is an emerging class of reinforcement learning (RL) algorithms that blend insights from Quality Diversity (QD) and RL to produce a collection of high performing and behaviorally diverse policies with respect to a behavioral embedding. Existing QD-RL approaches have thus far taken advantage of sample-efficient *off-policy* RL algorithms. However, recent advances in high-throughput, massively parallelized robotic simulators have opened the door for algorithms that can take advantage of such parallelism, and it is unclear how to scale existing off-policy QD-RL methods to these new data-rich regimes. In this work, we take the first steps to combine *on-policy* RL methods, specifically Proximal Policy Optimization (PPO), that can leverage massive parallelism, with QD, and propose a new QD-RL method with these high-throughput simulators and on-policy training in mind. Our proposed Proximal Policy Gradient Arborescence (PPGA) algorithm yields a 4x improvement over baselines on the challenging humanoid domain.

1 Introduction

Quality Diversity (QD) optimization is a class of algorithms that offers a principled way to combine exploitation with exploration in order to produce a collection of high performing and behaviorally diverse solutions. For example, a practitioner may want many policies that produce high-performing gaits, but vary in how they walk, skip, run, or limp to achieve that gait. The QD problem [4] considers an *objective* function $f(\cdot)$ to maximize and k *measure* functions $m_1(\cdot) \dots m_k(\cdot)$, which characterize the agent’s behavior. A QD algorithm aims to output a collection of solutions that maximize $f(\cdot)$ while being diverse w.r.t. these measure functions. Quality Diversity Reinforcement Learning (QD-RL) exploits the sequential decision making markov structure in the problem formulation to leverage RL to estimate gradients with respect to performance and diversity. QD-RL algorithms empower

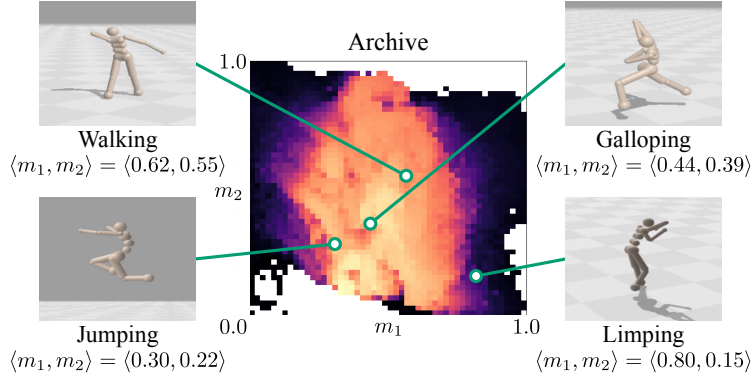


Figure 1: PPGA finds a diverse archive of high-performing locomotion behaviors for a humanoid agent by combining PPO gradient approximations with Differentiable Quality Diversity algorithms. The archive’s dimensions correspond to the measures m_1 and m_2 , i.e., the proportion of time that the left and right feet contact the ground. The color of each cell shows the objective value, i.e., how fast the humanoid moves. For instance, jumping moves the humanoid forward quickly, with the left and right feet individually contacting the ground 30% and 22% of the time, respectively.

practitioners to select from several high-performing policies for deployment after training, rather than being stuck with the final converged policy in traditional RL.

Current state-of-the-art QD-RL methods leverage off-policy RL, specifically TD3, and/or evolutionary strategies, to estimate the objective and measure gradients. These approaches reuse previously collected data to be sample efficient and make continuous improvements to the policies in the archive, and have shown great success in robotic locomotion and exploration tasks [37, 39, 48]. They are particularly useful in computationally constrained settings and benefit from faster sequential sampling. However, recent advances in GPU-Accelerated, high-throughput simulation [32, 17, 38] have led to a new paradigm for on-policy RL methods to take advantage of massive parallelism for high quality gradient estimates and faster wall-clock time convergence at the expense of sample-efficiency. Specifically, algorithms such as PPO [45] have shown great success in leveraging massive parallelism to solve increasingly more difficult simulated and real robotics tasks [40, 24, 2]. It is not clear how to bring existing QD-RL methods into this new training paradigm.

To date, there are no existing QD-RL methods that take advantage of this new data-rich regime, nor have there been attempts to combine on-policy RL methods with QD-RL to compare to existing off-policy QD-RL methods. In the QD-RL setting, not only is it important to provide high-quality performance and measure gradients for the algorithm to perform effectively, it is also important to leverage as much compute as is available since we wish to find a collection of high performing policies, as opposed to a single policy in the traditional RL setting. Therefore, we believe that the field of QD-RL would benefit from a method that leverages a highly parallelizable, on-policy RL algorithm to perform QD-RL optimization.

We observe that recent works in differentiable quality diversity (DQD) [12] algorithms – solving the first-order form of QD optimization – function in a manner highly synergistic with on-policy RL. State-of-the-art DQD algorithms maintain a *single search point* that explores one region of the behavioral embedding at a time. This local search is similar to how on-policy RL methods update from only local on-policy data. Prior methods [48] have attempted to combine off-policy RL with DQD. However, this ignores the local search nature of the DQD algorithm and does not scale to data-rich regimes. Thus, we hypothesize that on-policy RL, specifically PPO, will greatly outperform prior work that combines DQD algorithms with off-policy RL, due to the local search synergy.

Our key insight is to leverage parallel PPO implementations to accurately estimate on-policy objective and measure gradients. By leveraging massive parallelism to compute accurate gradients for a single search point, the DQD algorithm can then branch many nearby policies for parallel evaluation. The search forms a gradient arborescence that efficiently fills the behavioral embedding with diverse policies that each maximize their reward by amortizing the cost of the gradient approximation across many branched policies. Specifically, our work makes the following contributions:

1. We introduce the Proximal Policy Gradient Arborescence (PPGA) algorithm that leverages a modified, vectorized form Proximal Policy Optimization we call VPPO (Sec. 3) to estimate the objective and measure gradients, as well as, walk the policy in each ascending step of the gradient arborescence.
2. We view prior covariance matrix adaptation-based QD algorithms (in particular, CMA-ES-based) as instantiations of Natural Evolution Strategies (NES)-based methods and we propose combining QD with an alternative evolution strategy, xNES, that is more robust to the noise scale and non-stationarity typical of QD-RL tasks (Sec. 3).
3. We evaluate PPGA on four Quality Diversity locomotion domains built in Brax. In addition to achieving state-of-the-art results on all four domains, PPGA achieves a 4x improvement in performance in the high-dimensional humanoid domain (Sec. 4).

2 Prior Work

2.1 Deep Reinforcement Learning

Reinforcement Learning algorithms search for policies, a mapping of states to actions, that maximize cumulative reward in an environment. RL typically assumes the discrete-time Markov Decision Process formalism $(\mathcal{S}, \mathcal{A}, \mathcal{R}, \mathcal{P}, \gamma)$ where \mathcal{S} and \mathcal{A} are the state and action spaces respectively, $\mathcal{R}(s, a)$ is the reward function, $\mathcal{P}(s'|s, a)$ defines state transition probabilities, and γ is the discount factor. The RL objective is to maximize the discounted episodic return of a policy $\mathbb{E} \left[\sum_{k=0}^{T-1} \gamma^k R(s_k, a_k) \right]$ where T is episode length. **Deep Reinforcement Learning** solves the RL problem by finding a policy $\pi_\theta(a_t|s_t)$ parameterized by a deep neural network θ that represents the optimal state-action mapping.

On-policy Deep RL methods directly learn the policy π_θ using experience collected by that policy or a recent version thereof. Contemporary Actor-Critic methods [33] fit the value function $V_\phi(s_t)$ to discounted returns and estimate the advantage $\hat{A}_t = \sum_{k=t}^{T-1} \gamma^k R(s_k, a_k) - V_\phi(s_t)$, which corresponds to the value of an action over the current policy [44]. From here, the gradient of the objective w.r.t. θ , or **policy gradient**, can be estimated as $\hat{\mathbb{E}}_t \left[\nabla_\theta \log \pi_\theta(a_t|s_t) \hat{A}_t \right]$, and the policy π_θ is trained using mini-batch gradient descent.

Trust region policy gradient Deep RL methods constrain the policy updates to maintain the proximity of π_θ to the *behavior* policy $\pi_{\theta_{old}}$ which was used to collect the experience. TRPO [43] takes the largest policy improvement step that satisfies the strict KL-divergence constraint. Proximal Policy Optimization (PPO) [45] approximates the trust region approach by optimizing the clipped surrogate objective where $r_t(\theta) = \frac{\pi_\theta(a_t|s_t)}{\pi_{\theta_{old}}(a_t|s_t)}$ is the importance sampling ratio:

$$L(\theta) = \hat{\mathbb{E}}_{\pi_\theta} \left[\min(r_t(\theta) \hat{A}_t, \text{clip}(r_t(\theta), 1 - \epsilon, 1 + \epsilon) \hat{A}_t) \right]$$

Off-policy Deep RL algorithms learn parameterized state-action value functions $Q_\theta(s_t, a_t)$ that estimate the value of taking action a_t given state s_t . Greedy policy $\text{argmax}_a Q_\theta(s_t, a_t)$, or an ϵ -greedy variation thereof, generates actions. Q-functions can be learned from experience collected by recent or past versions of the policy or another policy altogether, hence the off-policy classification.

In continuous control problems, it can be difficult to find $a^* = \text{argmax}_a Q_\theta(s_t, a_t)$ due to an infinite number of possible actions. To work around this issue, off-policy methods such as DDPG [30] and TD3 [18] learn a deterministic policy $\mu_\phi(s_t)$ by solving $\text{max}_\phi(Q_\theta(s_t, \mu_\phi(s_t)))$ using gradient ascent.

2.2 Quality Diversity Optimization

Quality Diversity problems provide an *objective* function $f(\cdot)$ and k *measure* functions $m_1(\cdot) \dots m_k(\cdot)$, represented jointly as $\mathbf{m}(\cdot)$ [12], which defines an embedding the QD algorithm should span with diverse solutions. The **QD objective** is to find a solution which maximizes f for every possible output of \mathbf{m} . However, the embedding formed by \mathbf{m} is continuous, so the embedding space is discretized into a tessellation of M cells. The QD objective then becomes to maximize $\sum_{i=1}^M f(\theta_i)$, where θ_i is a solution whose measures $\mathbf{m}(\theta_i)$ fall in cell i of the tessellation. **Differen-**

Quality Diversity (DQD) [12] considers the first-order QD problem where the objective and measure functions are differentiable, with provided gradients represented as $\nabla f(\cdot)$ and $\nabla \mathbf{m}(\cdot)$.

QD algorithms originated with the NSLC [28, 29] and MAP-Elites [35, 8] algorithms. While these early QD algorithms were genetic algorithms, modern QD algorithms incorporate modern optimization techniques such as Bayesian optimization [26], evolution strategies [15, 7, 6], gradient ascent [12, 13], surrogate models [51, 3, 19], and differential evolution [5]. Several works have applied QD optimization to generative design [23, 20, 19], procedural content generation [22, 16, 9, 27, 46, 42, 41], human-robot interaction [11, 14], and robot manipulation [34].

2.3 Quality Diversity Reinforcement Learning

QD-RL focuses on the problem of producing a collection of high-performing and diverse *policies* by framing the sequential, decision making RL task as a QD optimization problem. Efficient methods for solving QD-RL problems approximate the gradients of both a policy’s performance and behavior via measure functions that map to a low dimensional behavioral embedding. These gradients are then combined with ideas from quality diversity optimization that maintain a diverse collection of solutions and drive the search towards discovering novel policies.

QD-RL methods can be roughly divided into two subgroups. The first set of approaches directly optimize over the entire archive by sampling existing policies in the archive and applying operations to the policies’ parameters that either improve their performance or diversity. For example, PGA-ME [37] collects experience from evaluated agents into a replay buffer and uses TD3 to derive a policy gradient that improves the performance of randomly sampled agents from the archive, while using genetic variation [50] on the same set of agents to improve diversity and fill new, unexplored cells. Similarly, QDPG [39] derives a policy and diversity gradient using TD3 and applies these operators to randomly sampled agents in the archive.

Whereas the first family of QD-RL algorithms simultaneously search the behavioral embedding in many different regions at once, the second family maintains a *single search policy* that explores new local regions one at a time. To efficiently populate the archive of diverse policies, the algorithm branches many policies from the current search policy by sampling different combinations of objective and measure gradients. A DQD algorithm then moves the search policy in the combination of objective and measure gradients that yielded the largest archive improvement according to the branched policies. In prior work [48], the authors considered objective gradient approximations via TD3 and OpenAI-ES, while approximating the measure function gradients with OpenAI-ES.

We note that the DQD formulation is closely aligned with the concept of on-policy RL. DQD algorithms maintain a single search policy from which new policies are branched, and moves this policy through the archive via gradient ascent towards underexplored regions, using only online data collected from the current search policy. Yet, none of the existing DQD-based QD-RL methods exploit this property. CMA-MAEGA(TD3, ES) uses off-policy RL despite the fact that old experience is used only to improve a single policy at a time, making it less efficient than PGA-ME. Furthermore, both CMA-MAEGA(TD3, ES) and separable CMA-MAE use evolutionary strategies to approximate either the objective and/or measure gradients, ignoring the Markov structure inherent in QD-RL problems. Finally, it is unclear how to scale either of the QD-RL method subgroups to highly parallelized, GPU-accelerated simulators given that all current methods use TD3, which is designed to be efficient for sequential RL. We aim to improve the the performance of DQD-based QD-RL

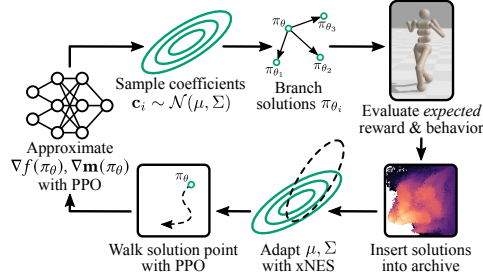


Figure 2: PPGA estimates $\nabla f, \nabla \mathbf{m}$ with PPO. We randomly sample gradient coefficients \mathbf{c} and perform weighted linear recombination of the objective-measure gradients with \mathbf{c} as the weights. This produces a population of gradients that in turn result in a population of branched policies. The policies are evaluated and inserted into the archive. xNES adapts the gradient coefficient distribution based on these insertions towards maximal archive improvement. The new mean of the coefficient distribution is used to walk the search policy towards a new, potentially unexplored region of the archive.

methods by integrating techniques from the on-policy RL literature that work well in these parallelized and data-rich regimes.

3 Proposed Method: The Proximal Policy Gradient Arborescence Algorithm

3.1 CMA-MAEGA

Our proposed PPGA algorithm builds off of the concept of a gradient arborescence first proposed by the DQD algorithm CMA-MEGA. Given a gradient basis matrix in objective-measure space, one can branch off policies in arbitrary directions in behavior embedding by weighting and linearly combining the gradient vectors in different ways. CMA-ES can then be applied to optimize for the optimal distribution of gradient coefficients, rather than the much higher dimensional policy parameter distribution. The arborescence is directed by ascending the QD objective in each search step determined by the distribution of gradient coefficients given by CMA-ES.

CMA-MEGA maintains a MAP-Elites archive that divides the k -dimensional embedding space into equally sized cells. To optimize for new candidate solutions, CMA-MEGA maintains a solution point in parameter space $\theta_\mu \in \mathbb{R}^N$ whose behaviors $m_1(\theta_\mu) \dots m_k(\theta_\mu)$ correspond to a position in the embedding. A DQD algorithm assumes access to gradients of the objective and measure functions. However, the optimal search direction depends on the state of the archive. To resolve this, CMA-MEGA maintains a CMA-ES instance that optimizes gradient coefficients for the objective and measure functions by maintaining a mean μ and covariance matrix Σ in the low dimensional embedding space $\mathbb{R}^{k+1} \ll \mathbb{R}^N$. In each step, we sample λ gradient coefficient vectors $\mathbf{c} \in \mathbb{R}^{k+1}$ to compute branching gradient steps. We linearly combine the objective and measure gradients to form each branching step: $\mathbf{c}\nabla g = c_0\nabla f + c_1\nabla m_1 + \dots + c_k\nabla m_k$. Each set of coefficients forms new candidate search positions: $\theta' = \theta_\mu + \mathbf{c}\nabla g$. From *one set* of objective and measure gradients, we sample λ new solutions for evaluation that vary in their objective and embedding position. We evaluate each solution θ' and compute the embedding $m_1(\theta'), \dots, m_k(\theta')$, which corresponds to some archive cell with an incumbent solution $\theta_{old}, f(\theta_{old})$ or a new unexplored cell whose $f(\theta_{old})$ is set to a minimum threshold. We rank the branched solutions according to the improvement on the objective $f(\theta') - f(\theta_{old})$, and CMA-ES steps μ, Σ in the direction of the natural gradient of the QD objective with respect to the gradient coefficients. CMA-MEGA steps the solution point θ_μ based on the log-likelihoods of the solutions with respect to the improvement ranking.

The state-of-the-art DQD algorithm CMA-MAEGA [13] introduced the concept of soft archives to CMA-MEGA. Instead of maintaining the best solution in each cell, the archive maintains a threshold t_e and updates the threshold by $t_e \leftarrow (1 - \alpha)t_e + \alpha f(\theta')$ when a new solution θ' crosses the threshold of its cell e . The hyperparameter $0 \leq \alpha \leq 1$ controls how quickly the soft archive changes. Soft archives have many theoretical and practical benefits discussed in prior work. Our proposed PPGA algorithm builds directly off the CMA-MAEGA algorithm.

3.2 Replacing CMA-ES with a Natural Evolution Strategy

Next, we motivate replacing CMA-ES with a Natural Evolution Strategy (NES) in PPGA. NES methods maintain a distribution in search space, parameterized by a Gaussian distribution. On each iteration, we sample search directions from the distribution $\phi = (\mu, \Sigma)$. Given an expected objective $J(\phi) \approx \frac{1}{n} \sum_{i=1}^n f(x_i)p(x_i|\phi)$, we compute the natural gradient $\nabla_\phi \mathbf{F}^{-1}(\phi)J(\phi)$ with respect to ϕ and step μ in the direction of the natural gradient and update Σ according to the observed curvature.

Prior works [21, 1] show that CMA-ES belongs in the NES family by constructing a bidirectional mapping between CMA-ES and NES updates. As both methods are natural gradient optimizers with invariance to order preserving transformations of f , we view CMA-MEGA and CMA-MAEGA as a instantiations of a general class of *Natural Evolution Strategy* DQD algorithms.

In this paper, we propose replacing CMA-ES with the Exponential Natural Evolution Strategy (xNES) [21], which makes several improvements over prior NES algorithms. Prior work [36] shows that CMA-ES’s cumulative step-size adaptation (CSA) mechanism is unstable in noisy and non-stationary RL domains. When developing the PPGA algorithm, we observed similar exploding step-size (σ) updates, which over time produced numerical errors and destabilized training. We

followed the recommendation of prior work [36] that showed the natural gradient step-size adaptation ($\nabla_{\sigma} = \text{tr}(\nabla_{\Sigma})/d$, $\Sigma \in \mathbb{R}^{d \times d}$) of xNES avoids such issues in RL domains.

3.3 Policy Gradients for Differentiable Quality Diversity Optimization

Unlike the standard QD formulation in which the analytical gradients of f and \mathbf{m} can be computed, the QD-RL setting considers the case in which these functions are non-differentiable and must be *approximated* with model-free RL. We formulate the control problem as a finite-horizon Markov Decision Process (MDP) over discrete time $(\mathcal{S}, \mathcal{A}, \mathcal{R}, \mathcal{P}, \gamma)$ and optimize the policy gradient objective $\nabla_{\theta} J(\theta) = \hat{\mathbb{E}}_t \left[\nabla_{\theta} \log \pi_{\theta}(a_t | s_t) \hat{A}_t \right]$.

PPO is an attractive choice as our gradient estimator because of its ability to scale with additional parallel environments, and it being an approximate trust region method provides some formal guarantees on the quality of the gradient estimates. This is particularly important in the QD-RL setting where the QD-objective is highly non-stationary. We utilize PPO to 1. estimate the gradients of the objective and measures ∇f , $\nabla \mathbf{m}$ and 2. move the search policy after μ, Σ have been adapted (we study the effect of this decision via ablation Sec. 4.3). We make several nontrivial modifications to the original PPO algorithm in order to adapt it to the QD setting, resulting in a new algorithm we call vectorized-PPO (VPPO). The details of this implementation, including how VPPO computes the objective-measure jacobian, are described in Appendix B. Of particular importance is making use of a fixed standard deviation parameter versus adaptive standard deviation. PPO employs a learned standard deviation parameter that parameterizes the action distribution on all agents, which decays over time and reduces the algorithm’s ability to explore in favor of converging more quickly to the optimal policy. In some environments, narrowing the action distribution can help with agent performance, whereas in others, it can hinder exploration and negatively impact our algorithm’s overall performance. To this end, we make adapting the standard deviation a configurable hyperparameter.

It is often the case that QD problems contain non-Markovian measure functions. For robot locomotion tasks, the standard measure function is the proportional foot contact time with the ground $m_i(\theta) = \frac{1}{T} \sum_{t=0}^T \delta_i(t)$ for each leg $i, i = 1..k$. However, this measure function is defined on a trajectory (i.e., the whole episode), making it non-Markovian and thus preventing us from using RL to estimate its gradient. To solve this issue, we introduce the notion of a **Markovian Measure Proxy** (MMP), which is a surrogate function that obeys the Markov property and has a positive correlation with the original measure function. For locomotion tasks, we can construct an MMP by simply removing the dependency on the trajectory and making the original measure function state-dependent, i.e., $m_i(s_t, a_t | \pi_{\theta}) = \delta_i(t)$, where the Kronecker delta $\delta_i(t)$ indicates whether the i ’th leg is in contact with the ground or not at time t . We can then use the exact same MDP as the standard RL formulation and replace the reward function with $m_i(s_t, a_t | \pi_{\theta})$.

Finally, instead of performing weighted recombination, we leverage the large quantities of on-policy data available to us in this data-rich regime to walk the search policy in the direction of greatest archive improvement using N_2 iterations of VPPO, where N_2 is a configurable hyperparameter. This choice is ablated in Sec. 4.3. Recall that the xNES update step produces a new mean and covariance matrix μ', Σ' in objective-measure gradient coefficient space. The updated mean gradient coefficients μ' describe a movement vector in the archive that will result in the greatest archive improvement. We use these coefficients to parameterize a new multi-objective reward function $R'(s_t, a_t | \pi_{\theta}) = c_0 R_{RL}(s_t, a_t | \pi_{\theta}) + \sum_{j=1}^k c_j m_j(s_t, a_t | \pi_{\theta})$. Optimizing this function with VPPO allows us to walk the search policy θ_{μ} in the direction of greatest archive improvement by iteratively taking conservative steps, where the magnitude of the movement is controllable by N_2 . We provide the full pseudocode in Algorithm 1.

4 Experiments

We evaluate our algorithm on four different continuous-control locomotion tasks derived from the original Mujoco environments [49]: Ant, Walker2d, Half-Cheetah, and Humanoid. The standard objective in each task is to maximize forward progress and robot stability while minimizing energy consumption. We use the Brax simulator to leverage GPU-acceleration and massive parallelization of the environments. The observation space sizes for these environments are 87, 17, 18, and 227, respectively, and the action space sizes are 8, 6, 6, and 17, respectively. The standard Brax

Algorithm 1 Proximal Policy Gradient Arborescence (PPGA)

Input: Initial solution θ_0 , VPPO instance to approximate $\nabla f, \nabla \mathbf{m}$ and move the search policy, number of QD iterations N_Q , number of VPPO iterations to estimate the objective-measure functions and gradients N_1 , number of VPPO iterations to move the search policy N_2 , branching population size λ , and an initial step size for xNES σ_g

Initialize the search policy $\theta_\mu = \theta_0$. Initialize NES parameters $\mu, \Sigma = \sigma_g I$

```
for iter  $\leftarrow$  1 to  $N$  do
   $f, \nabla f, \mathbf{m}, \nabla \mathbf{m} \leftarrow$  VPPO( $\theta_\mu, f, \mathbf{m}, N_1$ )
   $\nabla f \leftarrow$  normalize( $\nabla f$ ),  $\nabla \mathbf{m} \leftarrow$  normalize( $\nabla \mathbf{m}$ )
  update_archive( $\theta_\mu, f, \mathbf{m}$ )
  for  $i \leftarrow$  1 to  $\lambda$  do
     $c \sim \mathcal{N}(\mu, \Sigma)$ 
     $\nabla_i \leftarrow c_0 \nabla f + \sum_{j=1}^k c_j \nabla m_j$ 
     $\theta'_i \leftarrow \theta_\mu + \nabla_i$ 
     $f', *, m', * \leftarrow$  rollout( $\theta'_i$ )
     $\Delta_i \leftarrow$  update_archive( $\theta'_i, f', \mathbf{m}'$ )
  end for
  rank  $\nabla_i$  by  $\Delta_i$ 
  Adapt xNES parameters  $\mu = \mu', \Sigma = \Sigma'$  based on improvement ranking  $\Delta_i$ 
   $f'(\theta_\mu) = c_{\mu,0} f + \sum_{j=1}^k c_{\mu,j} m_j$ , where  $\mathbf{c}_\mu = \mu'$ 
   $\theta'_\mu =$  VPPO( $\theta_\mu, f', N_2$ )
  if there is no change in the archive then
    Restart xNES with  $\mu = 0, \Sigma = \sigma_g I$ 
    Set  $\theta_\mu$  to a randomly selected existing cell  $\theta_i$  from the archive
  end if
end for
```

environments are augmented with wrappers that determine the measures of an agent in any given rollout as implemented in QDax [31], where the number of measures of an agent is equivalent to the number of legs. The measure function is the number of times a leg contacts with the ground divided by the length of the trajectory. Our VPPO implementation used in PPGA is based on CleanRL’s implementation of PPO [25]. Most experiments were run on a SLURM cluster where each job had access to an NVIDIA RTX 2080Ti GPUs, 4 cores from a Intel(R) Xeon(R) Gold 6154 3.00GHz CPU, and 108GB of RAM. Some additional experiments and ablations were run on local workstations with access to an NVIDIA RTX 3090, AMD Ryzen 7900x 12 core CPU, and 64GB of RAM.

4.1 Comparisons

We compare our results to current state-of-the-art QD-RL algorithms: Policy Gradient Assisted MAP-Elites (PGA-ME) and Quality Diversity Policy Gradient (QDPG) implemented in QDax, and CMA-MAEGA(TD3, ES) implemented in pyribs. We also compare against the state-of-the-art ES-based QD-RL algorithm, separable CMA-MAE (sep-CMA-MAE) [47], which allows evolutionary QD techniques to scale up to larger neural networks. We use a standard grid archive with dimensions [10, 10, 10, 10] for Ant and [50, 50] for Walker2d, Half-Cheetah, and Humanoid. The same archive resolutions and network architectures are used for all baselines. A full list of shared hyperparameters is in Appendix A. We use an archive learning rate of 0.1, 0.15, 0.1, and 1.0 on Humanoid, Walker2d, Ant, and Half-Cheetah, respectively. Adaptive standard deviation is enabled for Ant as agents in this environment otherwise have trouble minimizing control cost. We reset the action distribution standard deviation to 1.0 on each iteration in all other environments.

PPGA consistently finds higher best-performing policies on all tasks. We completely outperform baselines on the Humanoid task on all metrics except coverage, achieving a 4x improvement over baselines on best reward. In all other tasks except ant, PPGA produces a policy distribution where most of the density lies in high performing regions of the archive as shown by the CDF plots. While PPGA does not achieve the highest QD scores and Coverage on every task, we argue that these metrics by themselves can be misleading, because one can fill all cells in the archive with low performing

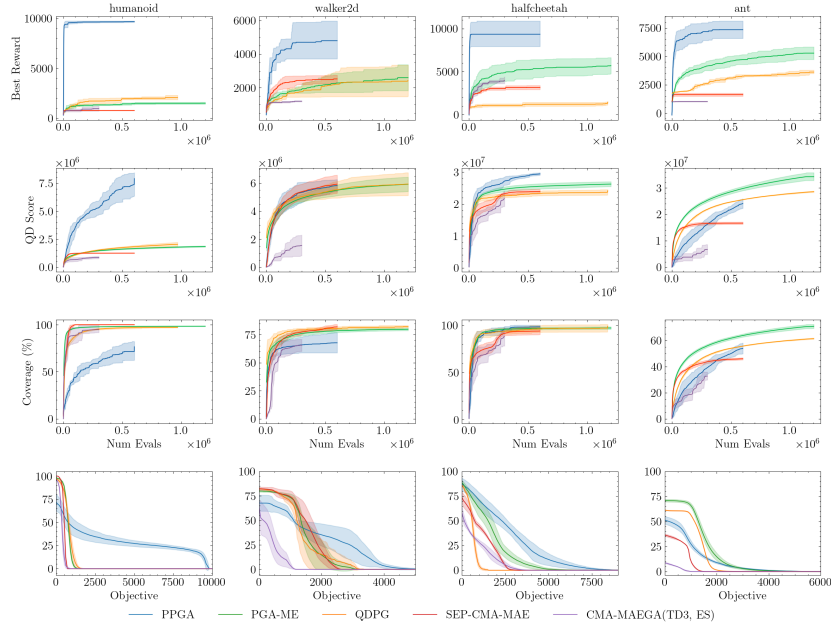


Figure 3: QD metrics and cumulative distributions for archives from PPGA compared to baselines. The CDF plots indicate the percentage of archive solutions that fall above a certain objective threshold. All plots are averaged over four seeds, and the shaded region represents +/- one standard deviation from the mean.

policies and achieve high scores for both metrics. The CDF plots encompasses both of these metrics, and provide insight into how the collection of policies is distributed w.r.t. performance. In all tasks but Ant, we achieve superior performance on this metric. PPGA struggles with high control cost penalties on Ant due to it using four legs to locomote, thus prompting us to enable adaptive standard deviation for this environment. Enabling adaptive standard deviation can result in worse performance as training progresses, since the action distribution converges and PPGA is no longer able to branch policies into new cells in the archive. This results in the lower coverage and QD-score as seen in Fig. 3. However, we are still able to find higher best-performing policies than the baselines.

All baselines generally outperform PPGA in coverage, with the exception of sep-CMA-MAE and CMA-MAEGA(TD3, ES) on Ant. Excluding QDPG, all baselines use some form of a genetic variation operator to improve diversity. We believe that this allows these algorithms to find cells in the archive that cannot be reached by following the gradients alone. However, it is often the case that agents produced by parameter space noise can get lucky and land in far-away cells, but these agents do not replicate, as we show in Sec. 4.2. Finally, QDPG has an explicit diversity operator, which allows it to be competitive with PPGA in terms of coverage, but is generally outperformed by PPGA on all other metrics.

4.2 Post-Hoc Archive Analysis

QD algorithms are known to struggle with reproducing performance and behavior in stochastic environments. To determine the replicability of our agents, we follow the guidelines laid out in [10]. That is, we re-evaluate each agent in the

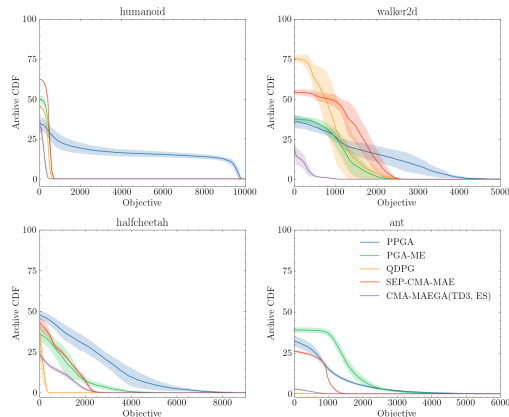


Figure 4: Corrected cumulative distributions, with +/- one standard deviation represented by the shaded regions.

archive 50 times and average its performance and measures to construct a Corrected Archive, and use this to produce Corrected QD metrics such as Corrected QD-Score and Corrected coverage. Table 1 and Fig. 4 show the corrected QD metrics and the corrected CDFs, respectively. After re-evaluating the archives, we find that the coverage gap significantly narrows, with PPGA even outperforming certain baselines such as PGA-ME in archive coverage on Half Cheetah. PPGA maintains overall higher performance, as indicated by the corrected CDF plots, and higher QD-Score, as indicated by the table, after re-evaluation on all tasks with the exception of Ant.

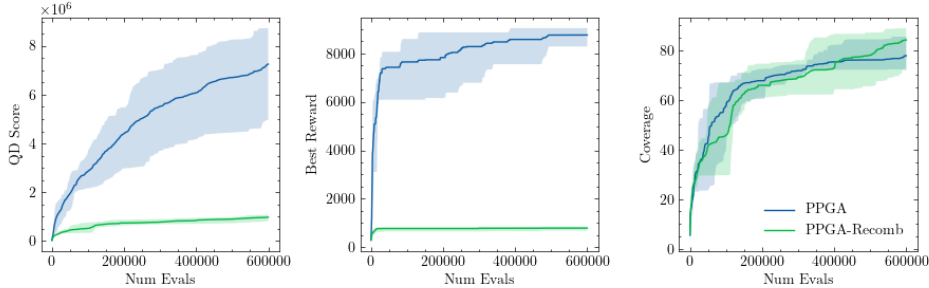


Figure 5: Ablation of walking the search policy with VPPO vs gradient recombination done in CMA-MEGA/CMA-MAEGA on the Humanoid environment.

4.3 Ablations

We compare walking the search policy with VPPO to using gradient recombination in the original formulation of CMA-MEGA. In addition, we ran an ablation of using xNES as the outer-loop optimizer compared to CMA-ES. However, the step-size adaptation parameter quickly diverges with CMA-ES and destabilizes training, and thus were unable to provide plots for this ablation. Fig. 5 shows the comparison of walking the search policy with VPPO versus using weighted linear recombination of the gradients. We believe that the large gap in performance is due to the fact that we can take multiple steps with VPPO via the N_2 hyperparameter. Weighted recombination results in a single gradient step where the updated search policy may land too close to the previous search policy’s cell. When we branch from the updated search policy, many branched agents will fall into overlapping cells, resulting in small archive improvement, which can lead to the emitter prematurely leaving a high-performing region of the search space.

5 Discussion and Limitations

We present a new method Proximal Policy Gradient Arborecence (PPGA) in which, for the first time, on-policy RL is applied to the DQD and QD-RL settings. We show that by leveraging an on policy RL algorithm that benefits from massive parallelism in GPU-accelerated simulators, we can achieve significant performance gains over baselines, most notably on Humanoid, a challenging, high-dimensional locomotion task. We generalize DQD algorithms that use covariance matrix adaptation as instantiations of Natural Evolution Strategies-based DQD methods and we propose using xNES as the outer-loop optimizer over gradient coefficient space, leading to significantly greater training stability. One caveat of using this approach is the sample complexity. Although parallelism allows for faster wall-clock time convergence, it does so at the expense of the algorithm’s sample efficiency. In data-constrained

Table 1: Corrected QD metrics

Algorithm	Exp.	QD-Score	Coverage	Best Reward
PPGA	Humanoid	4.11×10^6	34.49 %	9725
	Walker2d	2.68×10^6	35.81 %	4681
	Half Cheetah	1.51×10^7	49.55 %	8781
	Ant	1.47×10^7	33.55 %	7023
PGA-ME	Humanoid	5.93×10^5	50.16 %	714
	Walker2d	2.14×10^6	37.51 %	2037
	Half Cheetah	1.06×10^7	40.66 %	4867
	Ant	1.81×10^7	37.62 %	4582
sep-CMA-MAE	Humanoid	7.37×10^5	62.1 %	688
	Walker2d	3.88×10^6	54.21 %	2489
	Half Cheetah	1.4×10^7	55.67 %	2808
	Ant	1.15×10^7	29.83 %	1618
QDPG	Humanoid	5.91×10^5	49.9 %	715
	Walker2d	2.14×10^6	37.51 %	2038
	Half Cheetah	7.26×10^5	40.66 %	285
	Ant	3.05×10^6	25.21 %	789
CMA-MAEGA(TD3, ES)	Humanoid	1.94×10^5	33.57 %	467
	Walker2d	2.85×10^5	20.92 %	1057
	Half Cheetah	1.03×10^7	42.50 %	2773
	Ant	2.20×10^6	10.22 %	999

settings where not many parallel environments are available, PPGA's wall-clock time performance degrades as well. Nonetheless, we are excited to add this approach to the QD-RL family of algorithms. We are interested to see how this method scales to even more data-rich regimes such as distributed settings, as well as its application to harder problems such as real robotics tasks. We leave these as potential avenues of future research.

References

- [1] Youhei Akimoto, Yuichi Nagata, Isao Ono, and Shigenobu Kobayashi. Bidirectional relation between cma evolution strategies and natural evolution strategies. In Robert Schaefer, Carlos Cotta, Joanna Kołodziej, and Günter Rudolph, editors, *Parallel Problem Solving from Nature, PPSN XI*, pages 154–163, Berlin, Heidelberg, 2010. Springer Berlin Heidelberg. ISBN 978-3-642-15844-5.
- [2] Sumeet Batra, Zhehui Huang, Aleksei Petrenko, Tushar Kumar, Artem Molchanov, and Gaurav S. Sukhatme. Decentralized control of quadrotor swarms with end-to-end deep reinforcement learning. In Aleksandra Faust, David Hsu, and Gerhard Neumann, editors, *Conference on Robot Learning, 8-11 November 2021, London, UK*, volume 164 of *Proceedings of Machine Learning Research*, pages 576–586. PMLR, 2021. URL <https://proceedings.mlr.press/v164/batra22a.html>.
- [3] Varun Bhatt, Bryon Tjanaka, Matthew Fontaine, and Stefanos Nikolaidis. Deep surrogate assisted generation of environments. In S. Koyejo, S. Mohamed, A. Agarwal, D. Belgrave, K. Cho, and A. Oh, editors, *Advances in Neural Information Processing Systems*, volume 35, pages 37762–37777. Curran Associates, Inc., 2022. URL https://proceedings.neurips.cc/paper_files/paper/2022/file/f649556471416b35e60ae0de7c1e3619-Paper-Conference.pdf.
- [4] Konstantinos Chatzilygeroudis, Antoine Cully, Vassilis Vassiliades, and Jean-Baptiste Mouret. *Quality-Diversity Optimization: A Novel Branch of Stochastic Optimization*, pages 109–135. Springer International Publishing, Cham, 2021. ISBN 978-3-030-66515-9. doi: 10.1007/978-3-030-66515-9_4. URL https://doi.org/10.1007/978-3-030-66515-9_4.
- [5] Tae Jong Choi and Julian Togelius. Self-referential quality diversity through differential map-elites. In *Proceedings of the Genetic and Evolutionary Computation Conference, GECCO '21*, page 502–509, New York, NY, USA, 2021. Association for Computing Machinery. ISBN 9781450383509. doi: 10.1145/3449639.3459383. URL <https://doi.org/10.1145/3449639.3459383>.
- [6] Cédric Colas, Vashisht Madhavan, Joost Huizinga, and Jeff Clune. Scaling map-elites to deep neuroevolution. In *Proceedings of the 2020 Genetic and Evolutionary Computation Conference, GECCO '20*, page 67–75, New York, NY, USA, 2020. Association for Computing Machinery. ISBN 9781450371285. doi: 10.1145/3377930.3390217. URL <https://doi.org/10.1145/3377930.3390217>.
- [7] Edoardo Conti, Vashisht Madhavan, Felipe Petroski Such, Joel Lehman, Kenneth Stanley, and Jeff Clune. Improving exploration in evolution strategies for deep reinforcement learning via a population of novelty-seeking agents. In S. Bengio, H. Wallach, H. Larochelle, K. Grauman, N. Cesa-Bianchi, and R. Garnett, editors, *Advances in Neural Information Processing Systems 31*, pages 5027–5038. Curran Associates, Inc., 2018. URL <http://papers.nips.cc/paper/7750-improving-exploration-in-evolution-strategies-for-deep-reinforcement-learning-via-a-population-of-novelty-seeking-agents.pdf>.
- [8] Antoine Cully, Jeff Clune, Danesh Tarapore, and Jean-Baptiste Mouret. Robots that can adapt like animals. *Nat.*, 521(7553):503–507, 2015. doi: 10.1038/nature14422. URL <https://doi.org/10.1038/nature14422>.
- [9] Sam Earle, Justin Snider, Matthew C. Fontaine, Stefanos Nikolaidis, and Julian Togelius. Illuminating diverse neural cellular automata for level generation. In *Proceedings of the Genetic and Evolutionary Computation Conference, GECCO '22*, page 68–76, New York, NY, USA, 2022. Association for Computing Machinery. ISBN 9781450392372. doi: 10.1145/3512290.3528754. URL <https://doi.org/10.1145/3512290.3528754>.
- [10] Manon Flageat, Felix Chalumeau, and Antoine Cully. Empirical analysis of pga-map-elites for neuroevolution in uncertain domains. *ACM Trans. Evol. Learn. Optim.*, Jan 2023. ISSN 2688-299X. doi: 10.1145/3577203. URL <https://doi.org/10.1145/3577203>. Just Accepted.

- [11] Matthew Fontaine, Ya-Chuan Hsu, Yulun Zhang, Bryon Tjanaka, and Stefanos Nikolaidis. On the Importance of Environments in Human-Robot Coordination. In *Proceedings of Robotics: Science and Systems*, Virtual, July 2021. doi: 10.15607/RSS.2021.XVII.038.
- [12] Matthew C. Fontaine and Stefanos Nikolaidis. Differentiable quality diversity. In Marc’Aurelio Ranzato, Alina Beygelzimer, Yann N. Dauphin, Percy Liang, and Jennifer Wortman Vaughan, editors, *Advances in Neural Information Processing Systems 34: Annual Conference on Neural Information Processing Systems 2021, NeurIPS 2021, December 6-14, 2021, virtual*, pages 10040–10052, 2021. URL <https://proceedings.neurips.cc/paper/2021/hash/532923f11ac97d3e7cb0130315b067dc-Abstract.html>.
- [13] Matthew C. Fontaine and Stefanos Nikolaidis. Covariance matrix adaptation map-annealing. *CoRR*, abs/2205.10752, 2022. doi: 10.48550/arXiv.2205.10752. URL <https://doi.org/10.48550/arXiv.2205.10752>.
- [14] Matthew C. Fontaine and Stefanos Nikolaidis. Evaluating human–robot interaction algorithms in shared autonomy via quality diversity scenario generation. *J. Hum.-Robot Interact.*, 11(3), sep 2022. doi: 10.1145/3476412. URL <https://doi.org/10.1145/3476412>.
- [15] Matthew C. Fontaine, Julian Togelius, Stefanos Nikolaidis, and Amy K. Hoover. Covariance matrix adaptation for the rapid illumination of behavior space. In Carlos Artemio Coello Coello, editor, *GECCO ’20: Genetic and Evolutionary Computation Conference, Cancún Mexico, July 8-12, 2020*, pages 94–102. ACM, 2020. doi: 10.1145/3377930.3390232. URL <https://doi.org/10.1145/3377930.3390232>.
- [16] Matthew C. Fontaine, Ruilin Liu, Ahmed Khalifa, Jignesh Modi, Julian Togelius, Amy K. Hoover, and Stefanos Nikolaidis. Illuminating mario scenes in the latent space of a generative adversarial network. *AAAI Conference on Artificial Intelligence*, 35, February 2021. URL <https://ojs.aaai.org/index.php/AAAI/article/view/16740>.
- [17] C. Daniel Freeman, Erik Frey, Anton Raichuk, Sertan Girgin, Igor Mordatch, and Olivier Bachem. Brax - a differentiable physics engine for large scale rigid body simulation, 2021. URL <http://github.com/google/brax>.
- [18] Scott Fujimoto, Herke van Hoof, and David Meger. Addressing function approximation error in actor-critic methods. In Jennifer Dy and Andreas Krause, editors, *Proceedings of the 35th International Conference on Machine Learning*, volume 80 of *proceedings of machine learning research*, pages 1587–1596. pmlr, 10–15 jul 2018. URL <http://proceedings.mlr.press/v80/fujimoto18a.html>.
- [19] Adam Gaier, Alexander Asteroth, and Jean-Baptiste Mouret. Data-Efficient Design Exploration through Surrogate-Assisted Illumination. *Evolutionary Computation*, 26(3):381–410, 09 2018. ISSN 1063-6560. doi: 10.1162/evco_a_00231. URL https://doi.org/10.1162/evco_a_00231.
- [20] Adam Gaier, Alexander Asteroth, and Jean-Baptiste Mouret. Discovering representations for black-box optimization. In *Proceedings of the 2020 Genetic and Evolutionary Computation Conference, GECCO ’20*, page 103–111, New York, NY, USA, 2020. Association for Computing Machinery. ISBN 9781450371285. doi: 10.1145/3377930.3390221. URL <https://doi.org/10.1145/3377930.3390221>.
- [21] Tobias Glasmachers, Tom Schaul, Yi Sun, Daan Wierstra, and Jürgen Schmidhuber. Exponential natural evolution strategies. In Martin Pelikan and Jürgen Branke, editors, *Genetic and Evolutionary Computation Conference, GECCO 2010, Proceedings, Portland, Oregon, USA, July 7-11, 2010*, pages 393–400. ACM, 2010. doi: 10.1145/1830483.1830557. URL <https://doi.org/10.1145/1830483.1830557>.
- [22] Daniele Gravina, Ahmed Khalifa, Antonios Liapis, Julian Togelius, and Georgios N Yannakakis. Procedural content generation through quality diversity. In *2019 IEEE Conference on Games (CoG)*, pages 1–8. IEEE, 2019.
- [23] Alexander Hagg, Dominik Wilde, Alexander Asteroth, and Thomas Bäck. Designing air flow with surrogate-assisted phenotypic niching. In *International Conference on Parallel Problem Solving from Nature*, pages 140–153. Springer, 2020.

- [24] Ankur Handa, Arthur Allshire, Viktor Makoviychuk, Aleksei Petrenko, Ritvik Singh, Jingzhou Liu, Denys Makoviichuk, Karl Van Wyk, Alexander Zhurkevich, Balakumar Sundaralingam, Yashraj Narang, Jean-Francois Lafleche, Dieter Fox, and Gavriel State. Dextreme: Transfer of agile in-hand manipulation from simulation to reality. *arXiv*, 2022.
- [25] Shengyi Huang, Rousslan Fernand Julien Dossa, Chang Ye, Jeff Braga, Dipam Chakraborty, Kinal Mehta, and João G.M. Araújo. Cleanrl: High-quality single-file implementations of deep reinforcement learning algorithms. *Journal of Machine Learning Research*, 23(274):1–18, 2022. URL <http://jmlr.org/papers/v23/21-1342.html>.
- [26] Paul Kent and Juergen Branke. Bop-elites, a bayesian optimisation algorithm for quality-diversity search, 2020. URL <https://arxiv.org/abs/2005.04320>.
- [27] Ahmed Khalifa, Scott Lee, Andy Nealen, and Julian Togelius. Talakat: Bullet hell generation through constrained map-elites. In *Proceedings of The Genetic and Evolutionary Computation Conference*, pages 1047–1054, 2018.
- [28] Joel Lehman and Kenneth O. Stanley. Abandoning Objectives: Evolution Through the Search for Novelty Alone. *Evolutionary Computation*, 19(2):189–223, 06 2011. ISSN 1063-6560. doi: 10.1162/EVCO_a_00025. URL https://doi.org/10.1162/EVCO_a_00025.
- [29] Joel Lehman and Kenneth O. Stanley. Evolving a diversity of virtual creatures through novelty search and local competition. In *Proceedings of the 13th Annual Conference on Genetic and Evolutionary Computation*, GECCO '11, page 211–218, New York, NY, USA, 2011. Association for Computing Machinery. ISBN 9781450305570. doi: 10.1145/2001576.2001606. URL <https://doi.org/10.1145/2001576.2001606>.
- [30] Timothy P. Lillicrap, Jonathan J. Hunt, Alexander Pritzel, Nicolas Heess, Tom Erez, Yuval Tassa, David Silver, and Daan Wierstra. Continuous control with deep reinforcement learning. In Yoshua Bengio and Yann LeCun, editors, *4th International Conference on Learning Representations, ICLR 2016, San Juan, Puerto Rico, May 2-4, 2016, Conference Track Proceedings*, 2016. URL <http://arxiv.org/abs/1509.02971>.
- [31] Bryan Lim, Maxime Allard, Luca Grillotti, and Antoine Cully. Accelerated quality-diversity for robotics through massive parallelism. *arXiv preprint arXiv:2202.01258*, 2022.
- [32] Viktor Makoviychuk, Lukasz Wawrzyniak, Yunrong Guo, Michelle Lu, Kier Storey, Miles Macklin, David Hoeller, Nikita Rudin, Arthur Allshire, Ankur Handa, and Gavriel State. Isaac gym: High performance GPU based physics simulation for robot learning. In Joaquin Vanschoren and Sai-Kit Yeung, editors, *Proceedings of the Neural Information Processing Systems Track on Datasets and Benchmarks 1, NeurIPS Datasets and Benchmarks 2021, December 2021, virtual*, 2021. URL <https://datasets-benchmarks-proceedings.neurips.cc/paper/2021/hash/28dd2c7955ce926456240b2ff0100bde-Abstract-round2.html>.
- [33] Volodymyr Mnih, Adrià Puigdomènech Badia, Mehdi Mirza, Alex Graves, Timothy P. Lillicrap, Tim Harley, David Silver, and Koray Kavukcuoglu. Asynchronous methods for deep reinforcement learning. In Maria-Florina Balcan and Kilian Q. Weinberger, editors, *Proceedings of the 33rd International Conference on Machine Learning, ICML 2016, New York City, NY, USA, June 19-24, 2016*, volume 48 of *JMLR Workshop and Conference Proceedings*, pages 1928–1937. JMLR.org, 2016. URL <http://proceedings.mlr.press/v48/mniha16.html>.
- [34] Douglas Morrison, Peter Corke, and Jürgen Leitner. Egrad! an evolved grasping analysis dataset for diversity and reproducibility in robotic manipulation. *IEEE Robotics and Automation Letters*, 5(3):4368–4375, 2020. doi: 10.1109/LRA.2020.2992195.
- [35] Jean-Baptiste Mouret and Jeff Clune. Illuminating search spaces by mapping elites. *CoRR*, abs/1504.04909, 2015. URL <http://arxiv.org/abs/1504.04909>.
- [36] Nils Müller and Tobias Glasmachers. Challenges in high-dimensional reinforcement learning with evolution strategies. In Anne Auger, Carlos M. Fonseca, Nuno Lourenço, Pe-nousal Machado, Luís Paquete, and L. Darrell Whitley, editors, *Parallel Problem Solving from Nature - PPSN XV - 15th International Conference, Coimbra, Portugal, September 8-12, 2018, Proceedings, Part II*, volume 11102 of *Lecture Notes in Computer Sci-*

- ence, pages 411–423. Springer, 2018. doi: 10.1007/978-3-319-99259-4_33. URL https://doi.org/10.1007/978-3-319-99259-4_33.
- [37] Olle Nilsson and Antoine Cully. Policy gradient assisted map-elites. In *Proceedings of the Genetic and Evolutionary Computation Conference, GECCO '21*, page 866–875, New York, NY, USA, 2021. Association for Computing Machinery. ISBN 9781450383509. doi: 10.1145/3449639.3459304. URL <https://doi.org/10.1145/3449639.3459304>.
- [38] Aleksei Petrenko, Zhehui Huang, Tushar Kumar, Gaurav S. Sukhatme, and Vladlen Koltun. Sample factory: Egocentric 3d control from pixels at 100000 FPS with asynchronous reinforcement learning. In *Proceedings of the 37th International Conference on Machine Learning, ICML 2020, 13-18 July 2020, Virtual Event*, volume 119 of *Proceedings of Machine Learning Research*, pages 7652–7662. PMLR, 2020. URL <http://proceedings.mlr.press/v119/petrenko20a.html>.
- [39] Thomas Pierrot, Valentin Macé, Felix Chalumeau, Arthur Flajolet, Geoffrey Cideron, Karim Beguir, Antoine Cully, Olivier Sigaud, and Nicolas Perrin-Gilbert. Diversity policy gradient for sample efficient quality-diversity optimization. In *Proceedings of the Genetic and Evolutionary Computation Conference, GECCO '22*, page 1075–1083, New York, NY, USA, 2022. Association for Computing Machinery. ISBN 9781450392372. doi: 10.1145/3512290.3528845. URL <https://doi.org/10.1145/3512290.3528845>.
- [40] Nikita Rudin, David Hoeller, Philipp Reist, and Marco Hutter. Learning to walk in minutes using massively parallel deep reinforcement learning. In Aleksandra Faust, David Hsu, and Gerhard Neumann, editors, *Conference on Robot Learning, 8-11 November 2021, London, UK*, volume 164 of *Proceedings of Machine Learning Research*, pages 91–100. PMLR, 2021. URL <https://proceedings.mlr.press/v164/rudin22a.html>.
- [41] Anurag Sarkar and Seth Cooper. Generating and blending game levels via quality-diversity in the latent space of a variational autoencoder. *arXiv preprint arXiv:2102.12463*, 2021.
- [42] Jacob Schrum, Vanessa Volz, and Sebastian Risi. Cppn2gan: Combining compositional pattern producing networks and gans for large-scale pattern generation. In *Proceedings of the 2020 Genetic and Evolutionary Computation Conference*, pages 139–147, 2020.
- [43] John Schulman, Sergey Levine, Pieter Abbeel, Michael I. Jordan, and Philipp Moritz. Trust region policy optimization. In Francis R. Bach and David M. Blei, editors, *Proceedings of the 32nd International Conference on Machine Learning, ICML 2015, Lille, France, 6-11 July 2015*, volume 37 of *JMLR Workshop and Conference Proceedings*, pages 1889–1897. JMLR.org, 2015. URL <http://proceedings.mlr.press/v37/schulman15.html>.
- [44] John Schulman, Philipp Moritz, Sergey Levine, Michael I. Jordan, and Pieter Abbeel. High-dimensional continuous control using generalized advantage estimation. In Yoshua Bengio and Yann LeCun, editors, *4th International Conference on Learning Representations, ICLR 2016, San Juan, Puerto Rico, May 2-4, 2016, Conference Track Proceedings*, 2016. URL <http://arxiv.org/abs/1506.02438>.
- [45] John Schulman, Filip Wolski, Prafulla Dhariwal, Alec Radford, and Oleg Klimov. Proximal policy optimization algorithms. *CoRR*, abs/1707.06347, 2017. URL <http://arxiv.org/abs/1707.06347>.
- [46] Kirby Steckel and Jacob Schrum. Illuminating the space of beatable lode runner levels produced by various generative adversarial networks. In *Proceedings of the Genetic and Evolutionary Computation Conference Companion, GECCO '21*, page 111–112, New York, NY, USA, 2021. Association for Computing Machinery. ISBN 9781450383516. doi: 10.1145/3449726.3459440. URL <https://doi.org/10.1145/3449726.3459440>.
- [47] Bryon Tjanaka, Matthew C. Fontaine, Aniruddha Kalkar, and Stefanos Nikolaidis. Training diverse high-dimensional controllers by scaling covariance matrix adaptation map-annealing, 2022.

- [48] Bryon Tjanaka, Matthew C. Fontaine, Julian Togelius, and Stefanos Nikolaidis. Approximating gradients for differentiable quality diversity in reinforcement learning. In *Proceedings of the Genetic and Evolutionary Computation Conference, GECCO '22*, page 1102–1111, New York, NY, USA, 2022. Association for Computing Machinery. ISBN 9781450392372. doi: 10.1145/3512290.3528705. URL <https://doi.org/10.1145/3512290.3528705>.
- [49] Emanuel Todorov, Tom Erez, and Yuval Tassa. Mujoco: A physics engine for model-based control. In *2012 IEEE/RSJ International Conference on Intelligent Robots and Systems*, pages 5026–5033. IEEE, 2012. doi: 10.1109/IROS.2012.6386109.
- [50] Vassilis Vassiliades and Jean-Baptiste Mouret. Discovering the elite hypervolume by leveraging interspecies correlation. In *Proceedings of the Genetic and Evolutionary Computation Conference, GECCO '18*, page 149–156, New York, NY, USA, 2018. Association for Computing Machinery. ISBN 9781450356183. doi: 10.1145/3205455.3205602. URL <https://doi.org/10.1145/3205455.3205602>.
- [51] Yulun Zhang, Matthew C. Fontaine, Amy K. Hoover, and Stefanos Nikolaidis. Deep surrogate assisted map-elites for automated hearthstone deckbuilding. In *Proceedings of the Genetic and Evolutionary Computation Conference, GECCO '22*, page 158–167, New York, NY, USA, 2022. Association for Computing Machinery. ISBN 9781450392372. doi: 10.1145/3512290.3528718. URL <https://doi.org/10.1145/3512290.3528718>.

A Hyperparameters

Table 2: List of relevant hyperparameters for PPGA shared across all environments.

HYPERPARAMETER	VALUE
ACTOR NETWORK	[128, 128, ACTION DIM]
CRITIC NETWORK	[256, 256, 1]
N_1	10
N_2	10
PPO NUM MINIBATCHES	8
PPO NUM EPOCHS	4
OBSERVATION NORMALIZATION	TRUE
REWARD NORMALIZATION	TRUE
ROLLOUT LENGTH	128

B Vectorized-PPO Details

There are several key modifications to the original PPO implementation that were necessary to run PPO in an efficient manner within PPGA. Specifically, when computing the objective-measure Jacobian, $\langle \nabla f(\cdot) \in \mathbb{R}, \nabla \mathbf{m}(\cdot) \in \mathbb{R}^k \rangle$, the RL objective f and each measure function m are treated as separate single-objective optimization instances, where PPO optimizes each function one at a time. However, doing this sequentially would increase the runtime complexity by a factor of $k + 1$. To alleviate this issue, we designed a vectorized version of PPO, or **VPPO**. VPPO takes the current state of the agent, replicates it $k + 1$ times, and stores this in a **VectorizedActor** agent-class, which we will denote $\vec{\pi}_\theta$. Since PPO is an actor-critic method, we must also initialize $k + 1$ value functions $V_{\phi_1} \dots V_{\phi_{k+1}}$, one for each sub-actor in the vectorized agent. There is an additional value function V_{ϕ_μ} used when walking the mean solution point π_{θ_μ} that is independent of the Vectorized Actor. Thus, there are in total $k + 2$ value functions maintained over the lifetime of the program.

During the Jacobian computation phase, $\vec{\pi}_\theta$ is used to collect batched-rollouts over all N environments, where statistics such as advantage and return are computed only within $k + 1$ subgroups corresponding to the $k + 1$ subpolicies in the vectorized agent. VPPO then performs batch gradient descent to produce $\nabla f(\cdot), \nabla m_1(\cdot), \dots, \nabla m_{k+1}(\cdot)$, which are implicitly backpropagated to each sub-policy in $\vec{\pi}_\theta$ in a vectorized manner. This process is repeated for N_1 VPPO iterations, producing an updated vectorized actor $\vec{\pi}'_{\theta'}$. Then, the matrix $\vec{\pi}'_{\theta'} - \vec{\pi}_\theta$ i.e.

$$\begin{bmatrix} \pi'_{\theta_1} - \pi_{\theta_1} \\ \pi'_{\theta_2} - \pi_{\theta_2} \\ \dots \\ \pi'_{\theta_{k+1}} - \pi_{\theta_{k+1}} \end{bmatrix}$$

is the objective-measure Jacobian. The individual gradient vectors are normalized to be unit length before being used to branch new solutions off of the search policy.

When providing only a single objective to optimize such as when walking the mean solution point, VPPO simplifies and performs exactly as vanilla PPO.

C TD3GA Implementation Details

As part of our ablation study, we implemented TD3GA, which differs from PPGA by replacing all PPO mechanisms with TD3 [18]. This implementation required several algorithmic decisions, as PPGA was originally designed to integrate with an on-policy method like PPO rather than an off-policy method like TD3. In this section, we describe these decisions. In general, we intend our decisions to make TD3GA operate as closely as possible to PPGA, and we leave it to future work to explore whether variations of these decisions will further improve performance.

Algorithm 2 Vectorized-PPO (VPPO)

Input: Initial solution point π_{θ_i} , objective functions to optimize $\mathbf{f} = f_1(\cdot), \dots, f_k(\cdot)$, number of VPPO iterations N , number of parallel environments E , rollout length L

```
Initialize the vectorized agent  $\vec{\pi}_{\theta_i} = \text{vectorized\_agent}([\pi_{\theta}] \times (k + 1))$ 
for iter  $\leftarrow 1$  to  $N_1$  do
   $(\mathbf{S}, \mathbf{A}, \mathbf{R}, \mathbf{S}^*) \leftarrow \text{rollout}(\text{vectorized\_agent}, E, L, \mathbf{f})$  // Note that  $\mathbf{S} = \{S_1, \dots, S_k\}$ , etc
  advantage  $\mathbb{A}$ , returns  $\mathcal{G} \leftarrow \text{batch\_calculate\_rewards}(\mathbf{S}, \mathbf{A}, \mathbf{R}, \mathbf{S}^*, \mathbf{f})$ 
   $\vec{\pi}_{\theta}' \leftarrow \text{batch\_gradient\_descent}(\mathbb{A}, \mathcal{G}, \vec{\pi}_{\theta})$  // using the stochastic policy gradient
   $\vec{\pi}_{\theta} \leftarrow \vec{\pi}_{\theta}'$ 
end for
 $\nabla \mathbf{f} \leftarrow \vec{\pi}_{\theta}' - \vec{\pi}_{\theta_i}$ 
return  $\nabla \mathbf{f}$ 
```

Background: TD3 is an off-policy actor-critic method designed for single-objective RL tasks. TD3 maintains an actor (i.e., a policy) that takes actions in the environment, and a critic that estimates the action-value function. TD3 also maintains a replay buffer that stores experience collected by the actor. Over time, the actor is trained to optimize the critic. Simultaneously, based on experience in the replay buffer, the critic learns to better predict the action-value function.

Design Decisions:

1. **Number of critics:** In TD3GA, we maintain a TD3 critic for the objective function and one for each of the measure functions. We also create a separate critic for the weighted objective that is used when walking the solution point. We refer to these critics as the *objective* critic, *measure* critics, and *walking* critic.
2. **Choice of actor for critic training:** When training the critic, TD3 requires an actor that generates actions for states sampled from the replay buffer. Prior QD-RL methods that estimate objective gradients with TD3, e.g., PGA-ME [37] and CMA-MEGA (TD3, ES) [48], fulfill this role with a dedicated actor. This actor is referred to as a *greedy actor* since its primary purpose is to optimize its performance with respect to the critic.

In theory, since TD3 is an off-policy method, any actor, including a greedy actor, can be used to train the critic. However, to make TD3GA closer to PPGA, we instead use a copy of the current search policy to train the critic. This decision provides our TD3 instances with an on-policy nature that mirrors the PPO mechanisms found in PPGA.

3. **When to train critics:** Similar to the PPO value functions in PPGA, we maintain all critics throughout the entire training run, updating them on every iteration.
4. **Experience collection:** This decision concerns which experience collected in the environment should be inserted into the replay buffer. With the settings in our paper, PPGA (and TD3GA) samples 300 solutions per iteration, and each solution is evaluated for 10 episodes, with each episode having up to 1,000 timesteps of experience; in total, these solutions generate 3 million timesteps per iteration. The typical replay buffer size [18] in TD3 is 1 million, meaning the buffer would be filled three times over if we inserted all of this experience, i.e., the critic would never be trained with the experience from two-thirds of all solutions.

To ensure that we collect experience from many solutions across many iterations, we make two decisions. First, we only collect one episode of experience from each agent — this already cuts down experience collected on each iteration to 300,000 timesteps. Second, we increase the replay buffer size to 5 million to store experience across more iterations.

Note that there is no analogue to the replay buffer in PPGA, since PPO is an on-policy method. Instead, PPO regresses the value function based on experience collected while evaluating the solution point.

5. **Gradient computation:** We begin by describing how a prior method estimates the objective gradient with TD3. To estimate the objective gradient of a solution point, CMA-MEGA (TD3, ES) samples a batch of experience and passes the batch through the corresponding actor. The actions outputted by the actor are then inputted to the critic. Backpropagating through the critic and the actor then provides the objective gradient.

Roughly, the above procedure corresponds to taking a *single* step of TD3. However, in PPGA, the gradient is computed by taking the difference after *multiple* steps of PPO (the number of steps is determined by the hyperparameters N_1 and N_2). The straightforward approach to mirror this behavior in TD3GA is to also output a gradient after several steps of TD3. Thus, when training each critic, we also track the final state of the actor (recall that the actor used in critic training is a copy of the search policy). At the end of critic training, our gradient is then the difference between the final actor and the original search policy.

For example, to compute the objective gradient, we train the objective critic with an actor that is a copy of the search policy. While training the critic, the actor is updated so that it maximizes the objective critic. After N_1 steps, we compute the objective gradient as the difference between the actor and the original search policy.

6. **Actor target networks:** One TD3 mechanism that improved stability and performance was target networks, which are slowly updating versions of the actor and critic parameters. In TD3GA, it is straightforward to apply this mechanism to the critic parameters.

However, since the actor is reset to the current search policy on every iteration, it is difficult to maintain a single target network. Thus, on every iteration, the target network for the actor is simply reset to the current search policy’s parameters before the gradient computation.

Pseudocode: Algorithm 3 shows the process for computing an objective gradient in TD3GA. The same process applies to computing measure gradients. The process for walking the search policy is also similar, except that the reward is a weighted combination of the objective and measures (the weights come from the mean μ of the emitter’s coefficient distribution). Furthermore, when walking the search policy, we return the final actor instead of a gradient.

Hyperparameters: TD3GA inherits all relevant hyperparameters from PPGA (Table 2). It also inherits TD3 hyperparameters from prior QD-RL works that incorporate TD3 [48, 37], except for having a larger replay buffer. We also increase the batch size used during critic training to mimic the batch size used by PPO to regress the value function. Table 3 lists hyperparameters shared across all environments. Note that the archive learning rate depends on the environment but is identical to that used in PPGA.

Table 3: List of hyperparameters used in TD3GA, shared across all environments.

HYPERPARAMETER	VALUE
ACTOR NETWORK	[128, 128, ACTION DIM]
CRITIC NETWORK	[256, 256, 1]
TRAINING STEPS FOR OBJECTIVE AND MEASURES (N_1)	10
TRAINING STEPS FOR WALKING (N_2)	10
OPTIMIZER	ADAM
ADAM LEARNING RATE	3×10^{-4}
TARGET NETWORK UPDATE RATE (τ)	0.005
TARGET NETWORK UPDATE FREQUENCY (d)	2
SMOOTHING NOISE STANDARD DEVIATION (σ_p)	0.2
SMOOTHING NOISE CLIP (c)	0.5
DISCOUNT FACTOR (γ)	0.99
REPLAY BUFFER SIZE	5,000,000
BATCH SIZE (n_{batch})	48,000

Algorithm 3 TD3 Gradient Computation for the Objective. Adapted from TD3 [18]

Input: Current search policy params θ_μ , current TD3 critic networks Q_{ψ_1} and Q_{ψ_2} parameterized by ψ_1 and ψ_2 respectively, current critic targets ψ'_1 and ψ'_2 , replay buffer B

Hyperparameters: Training steps N_1 or N_2 , target network update rate τ , target network update frequency d , smoothing noise standard deviation σ_p , smoothing noise clip c , discount factor γ , batch size n_{batch}

Initialize actor $\phi = \theta_\mu$, actor target $\phi' = \theta_\mu$

{Either N_1 for gradient computation or N_2 for walking the search policy}

for iter $\leftarrow 1$ **to** N_1 **do**

{ r is replaced with the measures for measure gradients, or a weighted combination of the reward and measures for walking the search policy}

 Sample mini-batch of n_{batch} transitions (s, a, r, s') from B

{Train the critics}

$\tilde{a} \leftarrow \pi_{\phi'}(s') + \epsilon, \epsilon \sim \text{clip}(\mathcal{N}(0, \sigma_p), -c, c)$

$y \leftarrow r + \gamma \min_{i=1,2} Q_{\psi'_i}(s', \tilde{a})$

{This update is performed with Adam}

 Update critics $\psi_i \leftarrow \text{argmin}_{\psi_i} \frac{1}{N} \sum (y - Q_{\psi_i}(s, a))^2$

if $t \bmod d$ **then**

{Update ϕ by the deterministic policy gradient with Adam}

$\nabla_\phi J(\phi) = \frac{1}{n_{batch}} \sum \nabla_a Q_{\psi_1}(s, a)|_{a=\pi_\phi(s)} \nabla_\phi \pi_\phi(s)$

{Update target networks:}

$\psi'_i \leftarrow \tau \psi_i + (1 - \tau) \psi'_i$

$\phi' \leftarrow \tau \phi + (1 - \tau) \phi'$

end if

end for

{Note that $\psi_1, \psi_2, \psi'_1,$ and ψ'_2 are maintained across calls to this function}

{When walking the search policy, we just return the new policy params ϕ }

$\nabla f \leftarrow \phi - \theta_\mu$

return ∇f

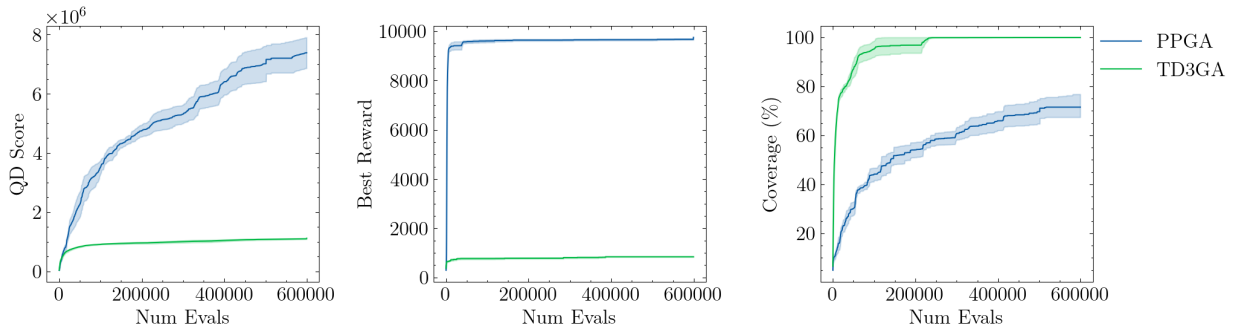


Figure 6: PPGA vs TD3GA on Humanoid. All plots are averaged over 4 seeds. The shaded region represents one standard deviation away from the mean.

D Hyperparameter Study

We investigate the effects of changing the N_1 and N_2 hyperparameters on the performance of PPGA in the Humanoid domain. We run 4 seeds of PPGA on the following combinations of N_1 and N_2 :

(10, 5), (5, 10), (5, 5), (1, 1) and compare against the baseline (10, 10). With these experiments, we wish to address the following questions

1. how few PPO steps on both the objective-measure jacobian calculation and walking the current search policy can we take before noticing performance degradation?
2. how do asymmetric choices for N_1 and N_2 (i.e. more jacobian calculation steps than walking steps and vice versa) affect performance?

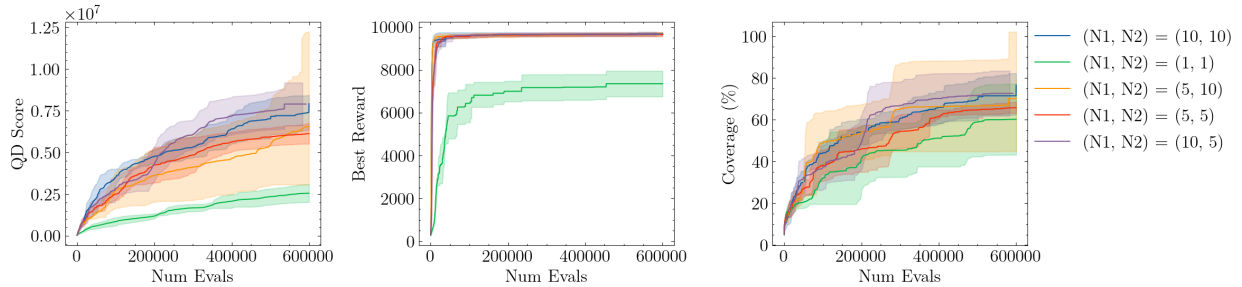


Figure 7: Study of the effect of different hyperparameter choices for N_1 and N_2 . N_1 is the number of PPO steps used to calculate the objective-measure jacobian, and N_2 is the number of PPO steps used to walk the search policy. All plots are averaged over 4 seeds. The shaded region indicates one standard deviation away from the mean.

(10, 5) achieves the most consistent results while achieving the same performance as the baseline, while (5, 10) results in very high run-to-run variance. This suggests that spending more compute on approximating the objective-measure jacobian is more important than walking the current search policy. (5, 5) achieves approximately 75% of the performance with half the computational expenditure when compared against the baseline. Thus, in a more computationally constrained setting, PPGA could be tuned to perform fewer N_1 and N_2 steps while still maintaining good performance. Finally, (1, 1) performs the worst, achieving only 25% of the baseline’s performance, implying that there is significant performance degradation when too few jacobian-calculation and walking steps are taken.